Thermochimica Acta 484 (2009) 32–37

Contents lists available at ScienceDirect

Thermochimica Acta

journal homepage: www.elsevier.com/locate/tca

A calorimetric study of solute effects on the kinetic stability of α-amylase

Søren N. Olsen[a], Kim B. Andersen[b], Lars H. Øgendal[c], Peter Westh[a,*]

[a] Roskilde University, Institute NSM, Functional Biomaterials, PO Box 260, 4000 Roskilde, Denmark
[b] Novozymes, Krogshoejsvej 36, 2880 Bagssværd, Denmark
[c] University of Copenhagen, Department of Basic Sciences and Environment, Thorvaldsensvej 40, 1871 Frederiksberg, Denmark

ARTICLE INFO

Article history:
Received 26 August 2008
Received in revised form
25 November 2008
Accepted 26 November 2008
Available online 11 December 2008

Keywords:
Isothermal titration calorimetry
Protein denaturation
Preferential interactions

ABSTRACT

In this study we evaluated the applications of isothermal titration calorimetry (ITC) to study solute effects on the kinetics of irreversible protein denaturation. More specifically, denaturation of *Bacillus Halmapalus* α-amylase (BHA) was initiated by addition of EDTA to the calorimetric cell, which reduces the thermostability of the protein from marginally stable to unstable at the experimental temperature, by removing bound calcium ions. The calorimetric signal was shown to be proportional to the unfolding rate of the protein, since, ΔH_{agg} was shown to be close to zero. Comparison of ITC with chromatographic size exclusion data (SEC) provided an avenue to study unfolding and aggregation separately, which proved to be useful in analysing the mechanism of solute effects on denaturation kinetics. Solute effects are discussed in line with preferential interactions and Wyman linkage function.

© 2008 Elsevier B.V. All rights reserved.

1. Introduction

Calorimetry has been extensively utilized to investigate the characteristic physical instability of proteins. A particularly prominent example is high sensitivity DSC, which is now the most important approach to characterize the reversible (equilibrium) unfolding of protein conformations. Recently, an increasing research interest has been directed towards kinetic protein stability; to the time course of irreversible denaturation processes such as aggregation or covalent modifications, which occur far from equilibrium [1]. This focus on kinetic stability is mostly driven by a strong interest in aggregated protein forms within the medical and pharmaceutical sciences. Aggregation is, for example, one of the major obstacles, which has to be overcome to market the numerous protein therapeutics which are currently in clinical trials [2]. Calorimetry has not yet been broadly applied in studies of kinetic protein stability, but some important progress has been made. The most straight forward approach is simply to follow the heat produced in a sample placed in an isothermal instrument. In many cases, it has been shown that the rate of irreversible break-down scaled with the heat flow (see [3] for a review), and hence that the kinetic stability could be monitored without specific knowledge about the qualitative nature of the irreversible process. This simplicity is often an advantage in technological applications, but a major limitation of the ITC approach is that it is only applicable to very slow processes (response time 20 s), and the requirement of a rather long thermal equilibration time (30 min). Scanning calorimetry has also been used in studies of kinetic protein stability. In this case the interpretation relies on non-linear regression with rather sophisticated models that takes in to account both thermodynamic and kinetic parameters [4,5]. In the current work we will test an ITC method which is an intermediate between the two other approaches. The basic idea, which was initially proposed by Nielsen et al. [6], is to keep the protein in the ITC cell under conditions where it is marginally stable, and then start an irreversible denaturation process through the titration of a destabilizing compound. Here we use a chelator, which removes stabilizing calcium ions from the investigated α-amylase, but other strategies such as pH jumps or addition of chemical denaturants also appear feasible. More specifically, we use this method to study solute effects on formation of so-called soluble (small) aggregates of the amylase. Thus we propose that the calorimetric method can be used as a screening tool, to evaluate solute effects on protein kinetic stability, which is an important process in protein formulation [7,8].

2. Experiments

2.1. BHA denaturation

The general experimental concept was to destabilize BHA by removing bound calcium ions from the protein (by addition of EDTA) thereby decreasing the thermostability to an extent so we could measure the kinetics of irreversible denaturation within a manageable time frame [6,9,10]. The basic calorimetric approach was adopted from [6]. All experiments were performed at 60 °C and the protein was destabilized by the addition of EDTA in molar ratio of 9 ([EDTA]/[BHA]).

* Corresponding author. Tel.: +45 46742879; fax: +45 46743011.
E-mail address: pwesth@ruc.dk (P. Westh).

0040-6031/$ – see front matter © 2008 Elsevier B.V. All rights reserved.
doi:10.1016/j.tca.2008.11.016

2.2. Protein and reagents

Recombinant *Bacillus halmapalus* α-amylase (BHA) was expressed in *Bacillus licheniformis* and purified to >95% (determined by SEC-MALLS and SDS PAGE). All buffers contained 20 mM HEPES (99%, Sigma, St Louis, US), 40 μM $CaSO_4$ (Sigma, St Louis, US) at pH 8 and varying concentrations of the following solutes: glycerol (0–1.5 M) (99%, Sigma, St Louis, US), sorbitol (0–1.5 M) (98% Sigma, St Louis, US), betaine (0–1.5 M) (98% Fluka, Buchs, CH), urea (0–1.5 M) (98% Sigma, St Louis, US), NaSCN (0–1.5 M) (98% Acros, New Jersey, US) and $(NH_4)_2SO_4$ (0–150 mM) (99%, Sigma, St Louis US).

2.3. Isothermal titration calorimetry (ITC)

Kinetics of BHA denaturation was followed using an ITC (VP-ITC, MicroCal, Northhampton, USA) at 60 °C. The protein solution (20 μM, ~1.1 mg ml^{-1}) was placed in the calorimetric cell (1.4 ml) and when the baseline had stabilized (600 s) BHA was titrated with 50 μl 5.2 mM EDTA (99%, Fluka, Buchs, CH) from the syringe. The stirring rate was 310 rpm and the titration duration was 14 s. Upon addition of EDTA, one or two of the three calcium ions that are bound to BHA are removed [9] resulting in a gradual protein denaturation. The heat flow of denaturation, which is proportional to the rate of denaturation (see below), was measured as a function of time. The raw data was deconvoluted according to Eq. (1) [6] using a non-linear regression routine, which returned maximum likelihood values for the 1st order rate constant of denaturation (k) and the enthalpy change ((H_{den}).

$$\frac{dq}{dt} = k\Delta H_{den} V[P]_0 e^{-kt} \quad (1)$$

In Eq. (1), dq/dt is the measured heat flow, $[P]_0$ the initial protein concentration, V the volume of the calorimetric cell and t the time after injection of EDTA.

2.4. Differential scanning calorimetry (DSC)

It is a requirement for the ITC procedures described above that the calcium saturated protein is (marginally) stable at the experimental temperature and that the chelator will change the stability so that some fraction of the protein unfolds. Thus, to find an appropriate temperature for the ITC measurements we estimated the thermal stability of BHA using a Nano DSC III (CSC, Lindon, Utah, USA) and a Scal-1 DSC (Scal Co., Pushchino, Russia) (no significant difference in the thermograms was observed between the two calorimeters). Prior to every experiment, baselines were measured filling the reference and sample cell with the same buffer. Thermograms were measured with a scan rate of 1 °C min^{-1} from 25 to 110 °C and the protein concentration was 20 μM. Thermograms were measured in either 1.5 M of glycerol, sorbitol, betaine, urea, NaSCN or in 150 mM $(NH_4)_2SO_4$. All of the above solute systems were measured with and without 182 μM EDTA corresponding to the concentration of EDTA in ITC experiments.

2.5. Size exclusion chromatography with UV detection (SEC-UV)

Aggregation kinetics was measured in solute systems equivalent to those analysed by ITC, quantifying the amount of monomeric protein as a function of time during aggregation. Ten ml BHA samples in 15 ml plastic centrifuge tubes were thermostated at 60 °C in a water bath. Upon addition of EDTA the sample was gently shaken, to ensure proper mixing of solutions. After addition of EDTA 1 ml sub samples were taken out in eppendorf tubes at regular time intervals and quenched by putting the eppendorf tubes on ice. Control experiments showed that the monomeric and aggregate protein pool remained constant over time (from quenching to SEC-UV analysis) at room temperature after quenching (measured by static light scattering, data not shown). Twenty to forty microliter aliquots of the quenched samples was injected on a Superose 6 column 10/300 GL (GE Healthcare, Uppsala, Sweden) and eluded at 0.5 ml min^{-1} using an Agilent 1100 HPLC (Agilent Technologies, Waldbronn, Germany). The elution buffer (50 mM borate, pH 9, adjusted with NaOH) passed through a UV detector (Beckman, Fullerton, CA), and the area of the monomeric protein peak was used to calculate the concentration of monomeric protein.

2.6. Theory

It has previously been shown that the main decay route for thermally denatured α-amylase is aggregation [11]. A simple, but often effective way to rationalize this type of process is the Lumry–Eyring model [12], which stipulates that the irreversible aggregation is preceded by a reversible structural change in the protein conformation.

$$N \underset{k_{-1}}{\overset{k_1}{\leftrightarrow}} U \xrightarrow{k_2} Ag \quad (2)$$

In Eq. (2), N, U and Ag are respectively native, unfolded (or partly unfolded) and aggregated protein. The rate constants k_1, k_{-1} and k_2 are defined in the usual way as indicated in the equation, so the equilibrium constant for the first step is $K = k_1/k_{-1} = [U]/[N]$. In the following we will refer to the first (equilibrium) step in Eq. (2) as *unfolding* (notwithstanding that significant components of residual structure may remain). The second step is *aggregation* while we will refer to the whole process of converting N to Ag as *denaturation*. The latter overall process is governed by an apparent rate constant k_{obs}.

Effects of added solutes on equilibria (such as the first step in Eq. (2)) may be rationalized through the theories of preferential interactions and linked equilibria [13,14]. The preferential interaction between solute and protein is usually expressed by the binding number (or the preferential binding parameter) which is defined:

$$\Gamma_{\mu_3} = \left(\frac{\partial m_3}{\partial m_2}\right)_{\mu_3} \quad (3)$$

where m denotes molal concentrations and subscripts 2 and 3 identify respectively protein and co-solute. The binding parameter reflects the binding stoichiometry measured in a conventional dialysis equilibrium experiment and may be either positive or negative depending on the relative affinity of water and solute for the protein surface. Negative Γ_{μ_3} for example (so-called preferential exclusion) implies favourable water–protein interactions (more so than solute–protein) and a concomitant local decrease of the solute concentration in the hydration shell of the protein. For many protein–solute systems, interactions have been found to be non-specific in the sense that Γ_{μ_3} scales approximately with the solvent accessible surface area (ASA) of the protein molecule [15]. Thus, the change, $\Delta\Gamma_{\mu_3}$, accompanying a conformational transition of the protein will be proportional to the change in surface area (ΔASA) [13,15–20]. According to Wyman linkage function, the effect on the previous mentioned equilibrium constant, K, of a solute with the thermodynamic activity a_3, may be written [14].

$$\frac{d\ln K}{d\ln a_3} = \Delta\Gamma_{\mu_3} \quad (4)$$

Hence, under this assumption of "non-specific" interactions, the effect of a solute on K may be estimated from the sign and size of Γ_{μ_3} for the native protein and the change in ΔASA. For example, equilibrium denaturation of a given protein results in an increase in ASA due to the partly unfolding of the polypeptide chain. Thus, as a direct consequence of the positive ΔASA, $\Delta\Gamma_{\mu_3}$ will be negative for excluded solutes since exclusion of the solute is proportional to

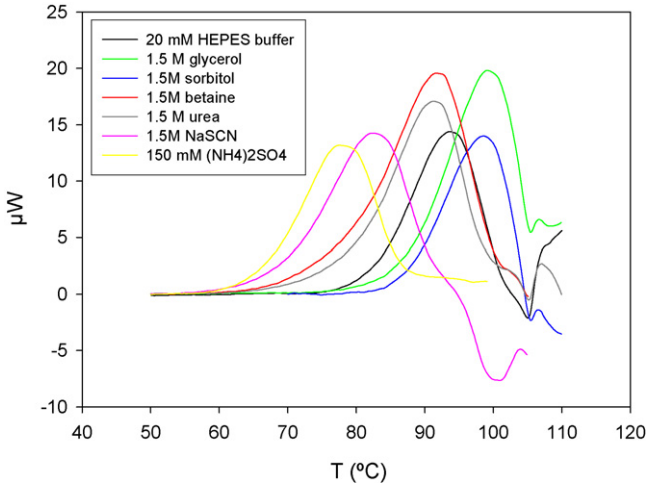

Fig. 1. DSC scans of native calcium saturated BHA in the different solute systems. The scan rate was 1 °C/min. The different solute systems are indicated in the upper left corner of the figure.

the surface area of the protein. This can be rationalized by considering preferential exclusion as stoichiometric "negative binding" (in a dialysis experiment), where binding of the solute is more negative for the denatured state compared to the native state. Therefore, according to Eq. (4) excluded solutes will stabilize the native state of proteins, while the opposite is true for preferentially bound solutes [13,17,20–26].

Clearly, Eqs. (3) and (4) are not immediately pertinent to the second (irreversible) step of Eq. (2). However, they may form the basis for our discussion as (i) they specify the equilibrium amount of U which is the reactant for the irreversible process and (ii) they may elucidate the transition state ($U^{\neq}$) which governs the rate of the second step [8,27,28].

3. Results

To find an appropriate temperature for the ITC measurements, the thermal stability of native calcium saturated BHA was measured by DSC. Selected results are shown in Fig. 1.

As seen from the figure, the apparent T_M (defined as the maximum in the DSC trace) varied significantly in the different solute systems, with the lowest value (~78 °C) for 150 mM $(NH_4)_2SO_4$ and the highest (~99 °C) for 1.5 M glycerol. No significant denaturation was observed at 60 °C in any of the solute systems as indicated by onset temperatures ≥60 °C for the peaks in Fig. 1. Denaturation was irreversible in all solute systems, since no peaks were observed in re-scans. The cause of irreversibility was due to aggregation/precipitation in the different solute systems indicated by the absence of a post-transitional baseline and the negative shift in heat flow at $T > T_M$. Upon addition of EDTA, T_M decreased to around 60 °C in 20 mM HEPES buffer, pH 8, but the thermograms were complex with multiple transitions (shoulders) and heavy aggregation at elevated temperature which precluded a precise determination of T_M (data not shown). However, based on the knowledge that calcium saturated BHA was stable and calcium depleted BHA unstable at 60 °C, ITC experiments were performed at this temperature, adding the chelator EDTA to the protein solution in the calorimetric cell (Fig. 2A).

Fig. 2A shows the raw data of a typical ITC experiment in 20 mM HEPES buffer at pH 8. After 600 s thermal equilibration (not shown), EDTA was injected into the calorimetric cell containing the protein solution (at $t = 0$ in Fig. 2). This resulted in a sharp exothermic peak (negative in Fig. 2A) followed by an endothermic and gradually decaying signal, showing the course of protein denaturation. The exothermic peak corresponds to binding of calcium to EDTA and the endothermic peak to denaturation of BHA [6]. The experimental enthalpy change was determined by integration of the positive denaturation endotherm (Fig. 2A). The post transitional baseline returned to the same heat flow as the pre-transitional baseline, and this level was simply subtracted from the raw data. The raw data was corrected for heat of dilution and heat of binding of Ca^{2+} to EDTA by performing a control experiment where EDTA was titrated into the buffer in the calorimetric cell containing 40 μM $CaCl_2$ without the presence of BHA (data not shown). The raw data was fitted using Eq. (1) (Fig. 2B) and the model accounted well for the data in all solutions, thus supporting the assumption of 1st order kinetics. Enthalpy changes derived from Eq. (1) was estimated to 1391 ± 51 (S.D.) kJ mol^{-1} ($n = 3$) which was close to the experimental measured enthalpy change of 1371 ± 30 kJ mol^{-1} ($n = 3$) (20 mM HEPES, pH 8).

To investigate if rate constants obtained from ITC correlated with aggregation rates, we studied the aggregation kinetics by SEC-UV, which provide an unambiguous quantification of the overall denaturation process. The kinetics of aggregate formation was measured as the decrease in weight concentration of monomers of BHA as a function of time. Examples of SEC-UV raw data for these measurements are presented in Fig. 3A. As seen from the figure, there were two distinct peaks in the UV signal during the aggregation

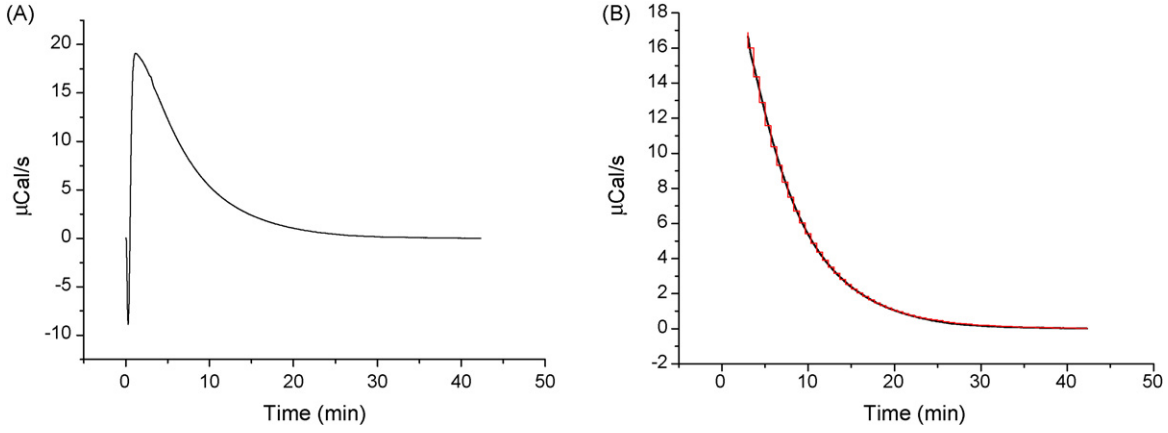

Fig. 2. ITC measurements of BHA denaturation. Panel A: Raw ITC data which show the heat flow of denaturation of 20 μM BHA at 60 °C, 20 mM HEPES, pH 8. The initial downward deflection (exotherm) is the heat of binding of Ca^{2+} to the chelator [6]. Panel B: Raw data (black solid line) and the best fit according to Eq. (1) (red step line) for the same trial as in panel A. The first 3 min of raw data was not used for fitting due to heat contributions from dilution and binding of calcium to EDTA. Data and fits are virtually indistinguishable. (For interpretation of the references to color in this figure legend, the reader is referred to the web version of the article.)

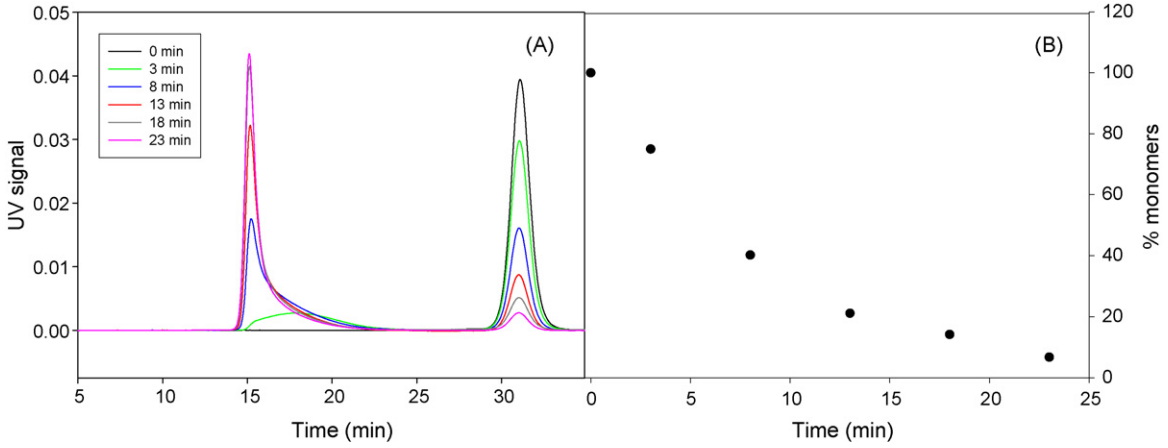

Fig. 3. Examples of SEC-UV data of quenched sub samples during aggregation in 20 mM HEPES buffer, pH 8. Panel A: UV signal as a function of elution time, after 0, 3, 8, 13, 18 and 23 min of aggregation at 60 °C. Panel B: Calculated percentage of monomers remaining as a function of time.

process. The first peak that eluded after approximately 15 min corresponds to soluble aggregates and the second peak, eluded after 32 min, corresponds to monomers.

In Fig. 3B the percentage of monomers remaining is plotted as a function of time, and the course of this curve was in accord with 1st order kinetics.

Fig. 4 shows rate constants obtained from ITC experiments plotted against rate constants measured by SEC-UV for the solutions that were investigated by both methods. It appears that all solutions except 1.5 M urea fall on a straight line with a slope close to unity (0.93) and a small intercept ($-0.0007\ s^{-1}$), strongly indicating that the ITC rate constants represents the overall denaturation rate constants ($N \rightarrow Ag$) for these solutions. In case of 1.5 M urea, on the other hand, the ITC rate constant is about four times larger than the SEC-UV rate constant. To illustrate this discrepancy further, we compared the time course of denaturation in 1.5 M urea as detected by the two methods. To this end the percentage of remaining monomeric protein was calculated from the ITC data as $(1\text{-}(Q(t)/Q_{total}) \times 100\%)$, where $Q(t)$ is the cumulative heat as a function of time and Q_{total} is the total heat of denaturation. This function is plotted against time in Fig. 5 together with the direct measurements of monomeric BHA by SEC-UV for 1.5 M urea and in 20 mM HEPES buffer.

As discussed below, the discrepancy (urea) or accordance (all solute systems except urea) of the two methods (Figs. 4 and 5), provides an avenue to analyse whether the solute effect on the overall denaturation process is related to the first or second step in Eq. (2).

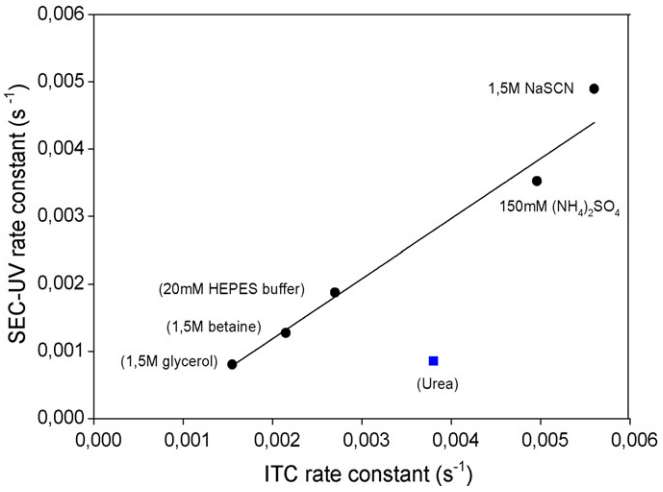

Fig. 4. Comparison between rate constants obtained from SEC-UV and ITC. Rate constant from SEC-UV are shown on the ordinate and represents the rate of aggregation. Rate constants from ITC measurements are shown on the abscissa. All data points except urea are fitted to a straight line with a slope of 0.93 and an intercept of $-0.0007\ s^{-1}$. The deviation of urea from this trend is discussed in the text.

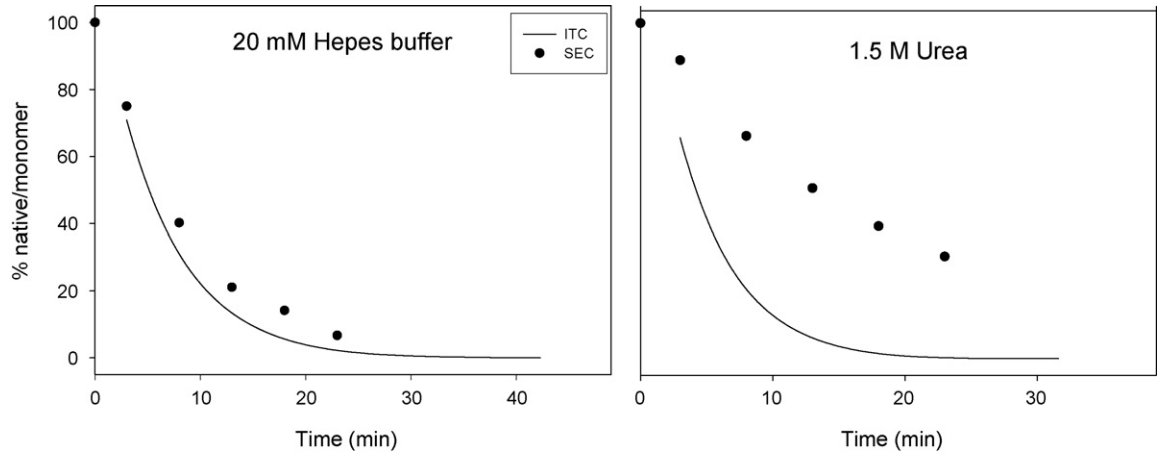

Fig. 5. Comparison between ITC and SEC-UV measurements of BHA aggregation in 20 mM HEPES and 1.5 M urea. The solid line represents ITC measurements and the solid circles SEC-UV measurements. The data indicates that ITC measures the rate of unfolding and SEC-UV measures the rate of aggregation.

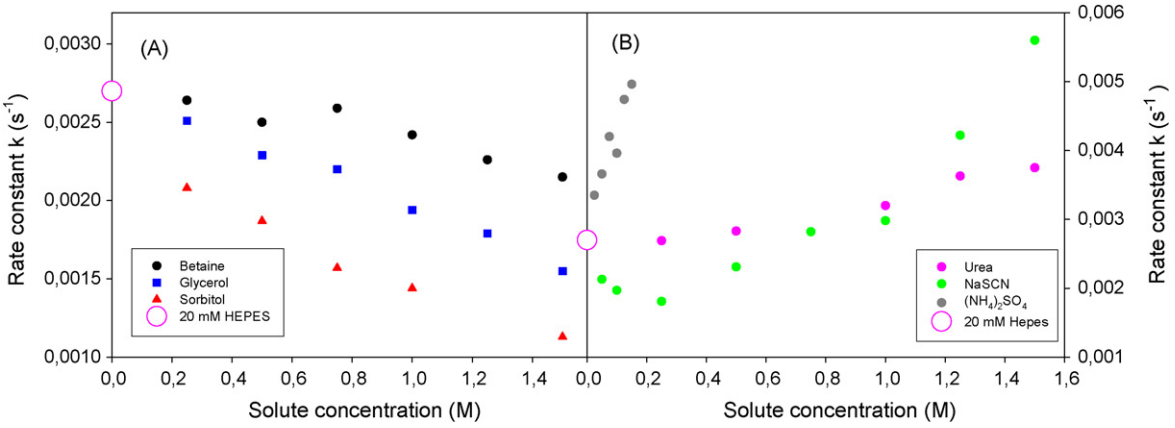

Fig. 6. ITC measurements of 1st order rate constants (k_{obs} in all systems except urea) of BHA denaturation as a function of solute concentration. Rate constants were derived from Eq. (1). Panel A: Glycerol (blue squares), sorbitol (red triangles), betaine (black circles). Panel B: Urea (pink circles, NaSCN yellow circles and $(NH_4)_2SO_4$ grey circles. (For interpretation of the references to color in this figure legend, the reader is referred to the web version of the article.)

Fig. 6 shows the effect of solute concentration on rate constants measured by ITC. For the preferentially excluded ($\Gamma_{\mu_3} < 0$) solutes glycerol, betaine and sorbitol [13,15], k_{obs} decreased in a near-linear fashion. In other words, these solutes promotes the colloidal stability of BHA (Fig. 6A). Glycerol and sorbitol seemed to be the best stabilizers, decreasing the rate constant of denaturation by approximately 50% at 1.5 M. Urea, which is a preferentially bound solute ($\Gamma_{\mu_3} > 0$) [29] had the opposite effect moderately increasing the rate constant (Fig. 6B). However, as seen from Fig. 5B, this rate constant does not describe the overall denaturation process, but rather the unfolding of the protein as discussed below.

Surprisingly $(NH_4)_2SO_4$ destabilized BHA, seen by the depression of melting temperatures in Fig. 1 and from the above ITC data, even though this salt is expected to be strongly excluded and thereby stabilize protein conformation [30,31]. The effect of NaSCN was complex in the sense that the salt kinetically stabilized BHA at low concentrations, but destabilized the protein at higher concentrations in accordance with the caotropic character of the salt [29,30]. Both salts induced visible (large) aggregates which were not observed for any of the organic solutes.

4. Discussion

4.1. Potential of the ITC method

The majority of multidomain proteins readily undergo irreversible transitions at physiological or industrially relevant solution conditions, and screening for improved protein shelf life, must therefore be based on reliable kinetic measurements of the rate limiting step in the process. Most experimental strategies rely on direct or indirect measurements of the concentration of reactant or product. Some important examples include fluorescence spectroscopy, SEC, light scattering or turbidity measurements. In contrast to these techniques, the current calorimetric approach directly detects the rate of the denaturation process (i.e. the derivative of concentration with respect to time). This eliminates errors associated with deriving rates from separate time-dependent concentration measurements and, together with the ease of use, appears to give the method a good potential for detailed kinetic analysis of protein denaturation. Compared to DSC, the method has the advantage of being isothermal, and thus not dependent on fitted or estimated values of the Arrhenius activation energy in the data analysis. The main limitations include the requirement to find an appropriate destabilizing compound, which can be titrated to the protein solution to start the process and the relatively high time constant of typical ITC instruments (20 s response time), which precludes investigations of fast denaturation.

The use of the ITC method in conjunction with other experimental approaches may be particularly effective in elucidating the rate determining step. An example of this is illustrated in Figs. 4 and 5. We suggest that the difference between urea and the other solutions reflects that SEC-UV (Fig. 3A) specifically detects the decay of monomers (i.e. the second step in Eq. (2)) while ITC quantifies the whole denaturation process weighted according to the enthalpy changes, ΔH_{unfold} and ΔH_{agg}, of each of the steps in Eq. (2). The decoupling of heat flow and monomer concentration for urea (Fig. 5) suggests that $\Delta H_{unfold} \gg \Delta H_{agg}$. Hence, at $t = 20$ min, for example, there is no measurable heat flow although the slope of the SEC-UV data shows an aggregation rate over 50% of the initial value. In the light of this and the linear relationship (with a slope close to unity (Fig. 4)) between the two experimental approaches in all other solutions than urea we conclude (i) that ITC essentially monitors the rate of the unfolding (first step in Eq. (2)) for the current systems, while it is insensitive to the second step because $\Delta H_{agg} \sim 0$, (ii) that the rate limiting step for the denaturation of BHA at 60 °C is unfolding in all solutions except urea (iii) and that urea changes the energy landscape in such a way that the aggregation step (Eq. (2)) becomes rate limiting. The second conclusion, which is substantiated by the essentially simultaneous unfolding (ITC) and aggregation (SEC-UV), is in accord with earlier investigations of other α-amylases [11]. The last conclusion is illustrated by the accumulation of BHA in the U-form (Fig. 5) and may be rationalized by the general observation of positive Γ_{μ_3} for urea [29]. In the simple "non-specific" view discussed above, this preferential binding of urea will accelerate the unfolding process (destabilize the native conformation) but impede the formation of a transition state, $U^{\neq}$, in the aggregation step, if $U^{\neq}$ is more compact that the U-form it self (which is likely for an aggregation process). This "dual effect" of denaturants on the colloidal stability of proteins has been discussed earlier for other systems [28,32].

4.2. Analysis of solute effects on BHA denaturation

As the denaturation rate for BHA was shown to be limited by the unfolding step in pure buffer without added solutes, a rather simple analysis of solute effects is possible. The overall rate constant of denaturation will be governed by the activation free energy for the unfolding process, $\Delta G^{\neq}_{unfold}$, and hence, the effect of the solutes will reflect their modification of this parameter. It is widely accepted that the native state is the most compact, and therefore it is likely

that ΔASA is positive and thus that excluded solutes will decrease the (rate limiting) unfolding rate. A simple calculation using Eq. (4), substituting the equilibrium constant with the transition state equilibrium constant ($K^{\neq}$), should give the difference in binding number and thereby the difference in ASA between the native state and the transition state. Using data of Γ_{μ_3}/ASA reported by Courtenay et al. [15], these calculations suggest an increase in ASA by 6%, calculated for the glycerol data in Fig. 6. Excluded solutes may also promote the production of the compact aggregated state (2. step in Eq. (2)), but since this process is already fast, denaturation rate will be unaffected by an increase in aggregation rate. Conversely, preferentially bound solutes may increase the rate of unfolding but decrease the rate of aggregation and hence (as in the case of urea in the current work) possibly shift the rate limiting step of denaturation from unfolding to aggregation. The above considerations are summarized as followed: excluded solutes can change the rate limiting step only when denaturation is aggregation limited in pure buffer. Conversely bound solutes can change the rate limiting step only when denaturation is unfolding limited in pure buffer. This interpretation is in accord with the data in as much as the non-electrolytes; glycerol, betaine and sorbitol, which have been shown to have negative Γ_{μ_3} for a number of other proteins [13,21] all promoted the kinetic stability of BHA whereas urea ($\Gamma_{\mu_3} > 0$) changed the process from unfolding limited to aggregation limited. However, the denaturation rates did not scale with the degree of preferential exclusion typically found for these solutes and other proteins. Betaine, for example, which is generally a strongly excluded solute had less effect on the overall rate of denaturation than the moderately excluded solute glycerol [15].

In contrast to the organic solutes, no correlation was found between the sign of Γ_{μ_3} and effects on colloidal stability for $(NH_4)_2SO_4$ and NaSCN. Thus both salts strongly destabilized BHA, even though $(NH_4)_2SO_4$ is expected to be preferentially exclude and NaSCN preferentially bound to the protein surface [29–31,33]. Such deviation of salt effects compared to organic solutes on irreversible protein aggregation has also been found by [28], and might represent a domination of electrostatic effects compared to preferential interactions. Possible mechanism may include direct binding of ions to protein surfaces [34–36] or charge shielding from counter ions affecting the chemical potential of proteins [30,37]. Thus the overall effect of a given salt will be the sum of the lyotropic and electrostatic effects, given rise to complex effects of the given salt. We suggest that these combined effects give rise to the observed dual effects of NaSCN, where the salt stabilized BHA at low concentrations and destabilized the protein at higher concentrations in accordance with the "salting in" nature of the salt [29,31] (Fig. 6B). The mechanism behind the decreasing structural (DSC and ITC, Figs. 1 and 6) and colloidal stability (SEC, Fig. 4) of $(NH_4)_2SO_4$ is not known and unexpected in the sense that $(NH_4)_2SO_4$ should be preferentially excluded from the protein. However, as pointed out by Arakawa et al. [35], preferential exclusion from the native state of proteins does not stabilize N in itself, if the given solute interacts more favourable with U (also seen from Eq. (4)). For example specific ion binding to U, combined with the general "salting out" character of $(NH_4)_2SO_4$ could explain the destabilizing effect of the salt. Furthermore both salts induced visible insoluble aggregates not seen for the organic solutes, which could be due to screening of surface charges decreasing the interaction potential of the formed aggregates as predicted by DLVO theory for colloidal stability [38].

5. Conclusion

In summary we concluded that ITC is a fast and reliable method to measure irreversible protein denaturation rates. Since the primary experimental observable in ITC is μW (μJ s^{-1}), ITC data is directly proportional to reaction rates seen by the agreement of ITC and SEC rate data when unfolding was rate limiting. Thus ITC provides a potential strong quantitative tool in the study of protein kinetic stability, which is of great importance in the pharmaceutical industry.

Acknowledgements

This work was supported by the Carlsberg Foundation, the Danish Research Agency (grants 26-02-0160 and 21-04-0087), the Danish National Research Foundation through the MEMPHYS, Center of Membrane Biophysics and the Danish Graduate School for Molecular Biophysics. Furthermore we want to thank Henrik Lund for inspiration by preliminary experiments.

References

[1] T.W. Randolph, J.F. Carpenter, AIChE 53 (2007) 1902–1907.
[2] B.S. Chang, S. Hershenson, in: J.F. Carpenter, M.C. Manning (Eds.), Rational Design of Stable Protein Formulations, Kluwer, New York, 2002, pp. 1–25.
[3] S. Gaisford, G. Buckton, Thermochim. Acta 380 (2001) 185–198.
[4] L.D. Creveld, W. Meijberg, H.J.C. Berendsen, H.A.M. Pepermans, Biophys. Chem. 92 (2001) 65–75.
[5] J.M. Sanchezruiz, J.L. Lopezlacomba, M. Cortijo, P.L. Mateo, Biochemistry 27 (1988) 1648–1652.
[6] A.D. Nielsen, C.C. Fuglsang, P. Westh, Biochem. J. 373 (2003) 337–343.
[7] J. Brange, in: S. Frökjaer, L. Hovgaards (Eds.), Pharmaceutical Formulation and Development of Peptides and Proteins, Taylor and Francis, London, 2000, pp. 89–112.
[8] E.Y. Chi, S. Krishnan, T.W. Randolph, J.F. Carpenter, Pharm. Res. 20 (2003) 1325–1336.
[9] A.D. Nielsen, M.L. Pusey, C.C. Fuglsang, P. Westh, Biochim. Biophys. Acta 1652 (2003) 52–63.
[10] M. Violet, J.C. Meunier, Biochem. J. 263 (1989) 665–670.
[11] C. Duy, J. Fitter, J. Biol. Chem. 280 (2005) 37360–37365.
[12] R. Lumry, H. Eyring, J. Phys. Chem. 58 (1954) 110–120.
[13] S.N. Timasheff, Biochemistry 41 (2002) 13473–13482.
[14] J. Wyman, S.J. Gill, Binding and Linkage, University Science Books, California, 1990.
[15] E.S. Courtenay, M.W. Capp, C.F. Anderson, M.T. Record, Biochemistry 39 (2000) 4455–4471.
[16] B.S. Kendrick, B.S. Chang, T. Arakawa, B. Peterson, T.W. Randolph, M.C. Manning, J.F. Carpenter, PNAS. US 94 (1997) 11917–11922.
[17] B.S. Kendrick, J.F. Carpenter, J.L. Cleland, T.W. Randolph, PNAS. US 95 (1998) 14142–14146.
[18] M.T. Record, W.T. Zhang, C.F. Anderson, Adv. Prot. Chem. 51 (1998) 281–353.
[19] S.N. Timasheff, Biochemistry 31 (1992) 9857–9864.
[20] S.N. Timasheff, Adv. Prot. Chem. 51 (1998) 355–432.
[21] K. Gekko, S.N. Timasheff, Biochemistry 20 (1981) 4677–4686.
[22] D.W. Bolen, I.V. Baskakov, J. Mol. Biol. 310 (2001) 955–963.
[23] Y.S. Kim, S.P. Cape, E. Chi, R. Raffen, P. Wilkins-Stevens, F.J. Stevens, M.C. Manning, T.W. Randolph, A. Solomon, J.F. Carpenter, J. Biol. Chem. 276 (2001) 1626–1633.
[24] E.Y. Chi, S. Krishnan, B.S. Kendrick, B.S. Chang, J.F. Carpenter, T.W. Randolph, Prot. Sci. 12 (2003) 903–913.
[25] F.G. Meng, Y.K. Hong, H.W. He, A.E. Lyubarev, B.I. Kurganov, Y.B. Yan, H.M. Zhou, Biophys. J. 87 (2004) 2247–2254.
[26] D.S. Katayama, R. Nayar, D.K. Chou, J.J. Valente, J. Cooper, C.S. Henry, D.G. Vander Velde, L. Villarete, C.P. Liu, M.C. Manning, J. Pharm. Sci. 95 (2006) 1212–1226.
[27] B.M. Baynes, B.L. Trout, Biophys. J. 87 (2004) 1631–1639.
[28] H.L. Bagger, L.H. Ogendal, P. Westh, Biophys. Chem. 130 (2007) 17–25.
[29] E.S. Courtenay, M.W. Capp, M.T. Record, Prot. Sci. 10 (2001) 2485–2497.
[30] P.H. Von Hippel, T. Schleich, in: S.N. Timasheff, G.D. Fasman (Eds.), Structure and Stability of Biological Macromolecules, Marcel Dekker, New York, 1969, pp. 417–569.
[31] T. Arakawa, S.N. Timasheff, Biochemistry 21 (1982) 6545–6552.
[32] T.B. Eronina, N.A. Chebotareva, N.B. Livanova, B.I. Kurganov, Biochem. Moscow 66 (2001) 449–455.
[33] R.L. Baldwin, Biophys. J. 71 (1996) 2056–2063.
[34] T. Arakawa, R. Bhat, S.N. Timasheff, Biochemistry 29 (1990) 1914–1923.
[35] T. Arakawa, R. Bhat, S.N. Timasheff, Biochemistry 29 (1990) 1924–1931.
[36] C.H.I. Ramos, R.L. Baldwin, Prot. Sci. 11 (2002) 1771–1778.
[37] C. Tandford, Physical Chemistry of Macromolecules, J. Wiley and Sons, Inc., New York, 1961.
[38] E.J.W. Verwey, J.TH.G. Overbeek, Theory of Lyophobic Colloids, Elsevier, New York, 1948.